Atmos. Chem. Phys., 11, 12627–12645, 2011
www.atmos-chem-phys.net/11/12627/2011/
doi:10.5194/acp-11-12627-2011

Atmospheric Chemistry and Physics

On aerosol hygroscopicity, cloud condensation nuclei (CCN) spectra and critical supersaturation measured at two remote islands of Korea between 2006 and 2009

J. H. Kim[1], S. S. Yum[12], S. Shim[2], S.-C. Yoon[3], J. G. Hudson[4], J. Park[5], and S.-J. Lee[5]

[1]Department of Atmospheric Sciences, Yonsei University, Seoul, Korea
[2]National Institute of Meteorological Research, Seoul, Korea
[3]School of Earth and Environmental Sciences, Seoul National University, Seoul, Korea
[4]Division of Atmospheric Sciences, Desert Research Institute, Reno, Nevada, USA
[5]National Institute of Environmental Research, Incheon, Korea

Received: 2 June 2011 – Published in Atmos. Chem. Phys. Discuss.: 11 July 2011
Revised: 18 November 2011 – Accepted: 25 November 2011 – Published: 15 December 2011

Abstract. Aerosol size distribution, total concentration (i.e. condensation nuclei (CN) concentration, N_{CN}), cloud condensation nuclei (CCN) concentration (N_{CCN}), hygroscopicity at ~90 % relative humidity (RH) were measured at a background monitoring site at Gosan, Jeju Island, south of the Korean Peninsula in August 2006, April to May 2007 and August to October 2008. Similar measurements took place in August 2009 at another background site (Baengnyeongdo Comprehensive Monitoring Observatory, BCMO) on the island of Baengnyeongdo, off the west coast of the Korean Peninsula. Both islands were found to be influenced by continental sources regardless of season and year. Average values for all of the measured N_{CCN} at 0.2, 0.6 and 1.0 % supersaturations (S), N_{CN}, and geometric mean diameter (D_g) from both islands were in the range of 1043–3051 cm^{-3}, 2076–4360 cm^{-3}, 2713–4694 cm^{-3}, 3890–5117 cm^{-3} and 81–98 nm, respectively. Although the differences in D_g and N_{CN} were small between Gosan and BCMO, N_{CCN} at various S was much higher at the latter, which is closer to China.

Most of the aerosols were internally mixed and no notable differences in hygroscopicity were found between the days of strong pollution influence and the non-pollution days for both islands. During the 2008 and 2009 campaigns, critical supersaturation for CCN nucleation (S_c) for selected particle sizes was measured. Particles of 100 nm diameters had mean S_c of 0.19 ± 0.02 % during 2008 and those of 81 and 110 nm diameters had mean S_c of 0.26 ± 0.07 % and 0.17 ± 0.04 %, respectively, during 2009. The values of the hygroscopicity parameter (κ), estimated from measured S_c, were mostly higher than the κ values obtained from the measured hygroscopic growth at ~90 % RH.

For the 2008 campaign, N_{CCN} at 0.2, 0.6 and 1.0 % S were predicted based on measured dry particle size distributions and various ways of representing particle hygroscopicity. The best closure was obtained when temporally varying and size-resolved hygroscopicity information from the HTDMA was used, for which the average relative deviations from the measured values were 28 ± 20 % for 0.2 % S (mostly under-prediction), 25 ± 52 % for 0.6 % (balanced between over- and under-prediction) and 19 ± 15 % for 1.0 % S (balanced). Prescribing a constant hygroscopicity parameter suggested in the literature ($\kappa = 0.3$) for all sizes and times resulted in average relative deviations of 28–41 % where over-prediction was dominant. When constant hygroscopicity was assumed, the relative deviation tended to increase with decreasing N_{CCN}, which was accompanied by an increase of the sub-100 nm fraction. These results suggest that hygroscopicity information for particles of diameters smaller than 100 nm is crucial for more accurate predictions of N_{CCN}. For confirmation when $\kappa = 0.17$, the average κ for sub-100 nm particles in this study, was applied for sub-100 nm and $\kappa = 0.3$ for all other sizes, the CCN closure became significantly better than that with $\kappa = 0.3$ for all sizes.

Correspondence to: S. S. Yum
(ssyum@yonsei.ac.kr)

Published by Copernicus Publications on behalf of the European Geosciences Union.

1 Introduction

The necessity to gain sufficient understanding of cloud condensation nuclei (CCN) has been increasing within the scientific community due to the realization that aerosol indirect effects that are initiated by anthropogenic emissions of CCN are imposing the greatest uncertainty in radiative forcing that is required for climate change predictions (IPCC, 2007; Schwartz et al., 2010). The CCN activity is controlled by the size of particles, the supersaturation (S) of the environment surrounding the aerosols, the dissolution behavior of the particle within the droplet and its surface tension (Pruppacher and Klett, 1997).

With the development and the dissemination of techniques such as differential mobility analyzers (DMA) (Knutson and Whitby, 1975), measurements of ambient aerosol number size distribution have increased in the last few decades, although the global coverage of such data is still far from sufficient (Kumala et al., 2004) and the effort to systematically combine surface measurement sites is only at its earliest stages only in the European region (Asmi et al., 2011).

Direct measurements of CCN are much scarcer due to the difficulty of the measurements and the lack of CCN instruments. Measuring the hygroscopicity of aerosols under subsaturated water vapor conditions has been suggested as a way to estimate CCN activity of aerosols (e.g. Brechtel and Kreidenweis, 2000; Kreidenweis et al., 2005). In those studies measured hygroscopicity was used to predict the critical supersaturation (S_c) or activation diameter (D_{p_act}) of particles, which is the threshold S or diameter, respectively, above which the thermodynamic equilibrium between the aerosols and the surrounding vapor collapses and the vapor condensation rate exceeds the evaporation rate. This leads to continuous growth of the particles, which are thus solution droplets. Recent development of a single parameter κ that incorporates Raoult's law and the Kelvin effect with the given value of surface tension of water made the quantitative comparison between hygroscopicity at sub-saturated condition and CCN activation more feasible (Petters and Kreidenweis, 2007).

For most of present day climate models, information on CCN number concentration (N_{CCN}) at specific S values is needed. To fulfill this requirement, many attempts have been made to retrieve N_{CCN} from aerosol hygroscopicity and size measurements at various regions such as subarctic (Kammermann et al., 2010), Amazon rainforest (Gunthe et al., 2009; Vestin et al., 2007; Zhou et al., 2002), coastal locations (Dusek et al., 2003; Kuwata et al., 2008), rural continental sites (Dusek et al., 2006; Gasparini et al., 2006) and large cities (Lance et al., 2009; Rose et al., 2010). Several authors have raised attention to the effect of the aerosol mixing state on N_{CCN} (Ervens et al., 2010; Wang et al., 2010; Wex et al., 2010). However, hygroscopicity data for ambient aerosols is still far from sufficient (Swietlicki et al., 2008). For S_c measurement of size-selected ambient particles only a few studies are available (Hudson and Da, 1996; Hämeri et al., 2001; Dusek et al., 2006; Hudson, 2007; Cerully et al., 2011).

In this study, we try to characterize hygroscopicity and S_c of aerosols measured in Asian continental outflow. Although several studies have investigated CCN and hygroscopic properties of the aerosols in this region (e.g. Adhikari et al., 2005; Eichler et al., 2008; Kuwata et al., 2008; Kuwata and Kondo, 2008; Massling et al., 2007, 2009; Matsumoto et al., 1997; Mochida et al., 2010; Rose et al., 2010; Wiedensohler et al., 2009; Yum et al., 2005, 2007), the scope of their spatial and temporal coverage was very limited despite the fact that the region has been under heavy industrial development for the last several decades. Here we present results from four different field campaigns that took place at western coastal sites of two remote islands near the Korean Peninsula (Fig. 1) from 2006 to 2009.

2 Measurement and campaign description

2.1 Gosan, Jeju Island

On Gosan, Jeju Island two measurement shelters (about 10 m apart) located at the top of a cliff (33.2° N, 126.1° E, 70 m above sea level, Fig. 1) were used. Since local sources near this site are limited, it has served as a supersite for several international campaigns, including ACE-ASIA (Hubert et al., 2003), ABC-EAREX2005 (Nakajima et al., 2007), Pacific Dust Experiment (PACDEX) (Stith et al., 2009) and Cheju ABC Plume-Asian Monsoon Experiment (CAPMEX) (Ramana et al., 2010).

The measurements took place during three periods: 15 August–1 September 2006 (hereafter denoted as Gosan 2006); 14 April–16 May 2007 (Gosan 2007); 1 August–11 October 2008 (Gosan 2008). A TSI condensation particle counter (CPC) 3010 was used to measure total number concentration of particles (i.e. condensation nuclei (CN) concentration, N_{CN}). A separate SMPS system, which has its own CPC as a component, measured the size distributions of particles of diameters 10–470 nm. Sample air for the SMPS was not dried except during Gosan 2008. For CCN number concentration (N_{CCN}) measurements, the Desert Research Institute Instantaneous CCN Spectrometers (CCNS) (Hudson, 1989) were used for Gosan 2006 and a Droplet Measurement Technologies (DMT) CCN counter (CCNC) (Roberts and Nenes, 2005) was used in all of the other campaigns.

CCNS was calibrated everyday during Gosan 2006 with monodisperse ammonium sulfate particles. CCNC was calibrated with monodisperse sodium chloride particles after the Gosan 2006 campaign, following the procedure similar to that explained by Rose et al. (2008). The main purpose of the CCNC calibration was to take into account atmosphere pressure difference between the manufacturer location (840 mb) and Gosan (1000 mb) and the calibration result was applied to Gosan 2007 and Gosan 2008. Another

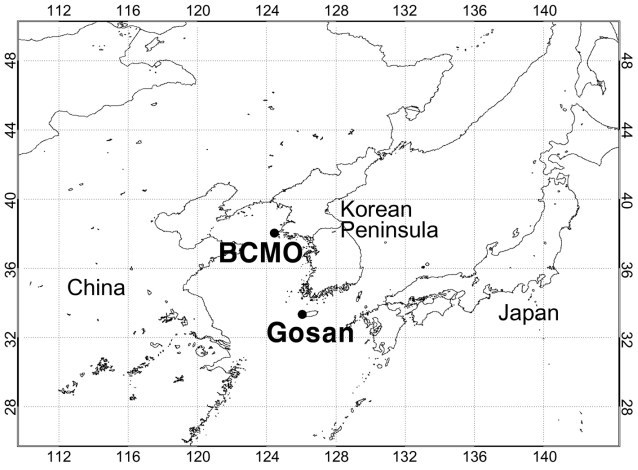

Fig. 1. Locations of the measurement sites, Gosan and BCMO (Baengnyeongdo Comprehensive Monitoring Observatory).

CCNC calibration was done before BCMO 2009, again with monodisperse NaCl particles and there was a small calibration drift. What had previously been 0.2, 0.4, 0.6, 0.8 and 1.0 % S was then 0.19, 0.42, 0.66, 0.89 and 1.13 % S, respectively after the experiment. Note that the differences were especially small for the S_c range 0.2–0.4 %, where most of the measured S_c lies as will be shown later. For both CCNS and CCNC, the Köhler model denoted as analytical approximation 1 (AA1) by Rose et al. (2008) was used to obtain S_c of the particles.

Although N_{CCN} from CCNS was mainly used for Gosan 2006, CCNC was also available for a short period (6 days) during that campaign. For this overlapping period, N_{CCN} from CCNS was −14 %, −4 %, 4 % and 6 % higher than N_{CCN} from CCNC at 0.35 %, 0.52 %, 0.69 % and 0.86 % S, respectively. The coefficient of determination (r^2) for 1 h-averaged N_{CCN} was 0.77, 0.81, 0.89 and 0.85, respectively, for these S.

Hygroscopic growth factors for dry particles between 50 and 250 nm were measured by a typical humidified tandem differential mobility analyzer (HTDMA). RH was measured by 3 capacity-type RH sensors either from Vaisala (model HMM22d, uncertainty of ±2 %RH) or Testo (model 06369735 and model 06369740, uncertainty of ±2 %RH) at the exits of the first DMA, the nafion humidifier and the sheath air of the second DMA. These RH sensors were calibrated by the local distributors of the instruments before each campaign. Hygroscopicity measurements were done only for several hours of each day during Gosan 2006 while hygroscopicity measurements were continuous during Gosan 2007 and 2008.

The mass concentration for particles smaller than 10 µm (PM_{10}) and 2.5 µm ($PM_{2.5}$) and gas concentrations of sulfur dioxide (SO_2), carbon monoxide (CO), ozone (O_3), nitrogen dioxide (NO_2) were measured with Met One BAM1020, Met One FH-62, TEI 43C-TL, TEI 48C, TEI 49C and TEI 42CTL, respectively, at the second shelter maintained by NIER.

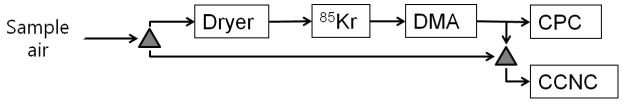

Fig. 2. Configuration of instruments for measuring N_{CCN} and characterizing S_c during Gosan 2008 and BCMO 2009. The grey triangles represent 3-way valves.

S_c of monodisperse particles of selected sizes were measured along with N_{CCN} during Gosan 2008 by the configuration shown in Fig. 2. The 3-way valves controlled whether the sample air followed the upper or lower branches in Fig. 2.

For each S, the sample air was first led to the lower branch for 180 s when N_{CCN} for polydisperse aerosol was measured. Only the polydisperse N_{CCN} data from the last 30 s was used so that CCNC had completed the S transition from the previous setting. Next, the sample air was led to the upper branch where it went through a dryer, aerosol neutralizer and DMA before reaching the CPC and CCNC. DMA selected monodisperse dry diameters (D_{dry}) were 50, 100 and 200 nm, although 200 nm data was not used in this study. For each size 85 s were consumed but only data from the last 30 s was used. After the monodisperse N_{CCN} measurements for three sizes were completed, the instrument proceeded to the next S and repeated the aforementioned procedure. When all 11 S measurements were completed, an extra 480 s were assigned to stabilize S since CCNC then had to change from the highest S to the lowest S. Therefore, it took approximately 86 min to obtain one complete CCN spectrum.

The resulting size-segregated N_{CCN} to N_{CN} ratios were plotted against 11 S points between 0.06 % and 0.8 % S (Fig. 3). S_c was then identified as the S at which the height of the fitted sigmoid curve was the half of the maximum height. In order to take into account multiply charged aerosols, which would create a small hill at lower S, the sigmoid curve was allowed to have a non-zero y-intercept. During Gosan 2006 and Gosan 2007, this configuration was not used and both DRI CCNS and DMT CCNC measured only ambient N_{CCN} in polydisperse mode.

2.2 BCMO, Baengnyeongdo

Similar measurements took place at Baengnyeongdo Comprehensive Monitoring Observatory (BCMO) (about 150 m above sea level; 38.0° N, 124.6° E) on the island of Baengnyeongdo (Fig. 1) during 5 August–30 August 2009 (BCMO 2009). The local sources near that site were also very limited and BCMO served as a background air quality monitoring station. The CCNC configuration in Fig. 2, TSI CPC 3010 and HTDMA were again used. This time

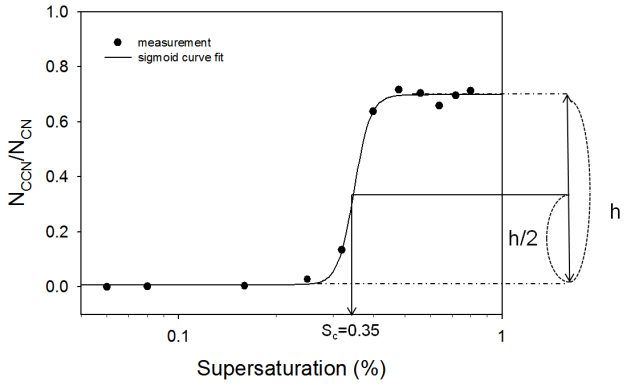

Fig. 3. Example of S_c characterization for 100 nm dry particles.

N_{CCN}/N_{CN} was measured at 12 S points between 0.07 % and 1.3 % S and the time needed for a complete CCN spectrum was 76 min. The aerosol size distribution was measured only for the last 3 days by TSI SMPS 3936L10. CCNC was calibrated by a similar process as stated above.

PM_{10}, $PM_{2.5}$, SO_2, CO, O_3, NO_2 were also measured with Thermo 1400A, Thermo 1405, Teledyne 100A, Teledyne 300EU, Teledyne 400E and Teledyne 200AU, respectively.

3 Results

3.1 PM and gaseous species concentrations

Based on the daily average PM_{10}, $PM_{2.5}$, SO_2, O_3, CO, NO_2 (or NO_y for BCMO 2009) concentration data, days with significant pollution were identified for each campaign. Such days were 17, 18 and 28 August 2006; 26, 27 April and 7 and 8 May 2007; 18–22 August and 30 September –11 October 2008; and 13–16 August 2009. Relatively higher concentrations of SO_2 and O_3 were general characteristics of the pollution periods and high $PM_{2.5}$ and PM_{10} concentrations were also found in all pollution periods except for the later pollution period in 2008. It should be noted that the distinction between pollution and non-pollution days is relative. For example, according to the Flower et al. (2010) classification of pollution periods based on optical and chemical composition measurement of aerosols at the Gosan site, 74 % of the days in August and September 2008 were designated pollution days. The pollution periods classified in this study were only a minor fraction of that pollution period.

Figure 4 shows average particle and gaseous concentrations for each classification. Gosan 2007 generally showed the highest concentrations for most species and the highest for all species for pollution periods. Meanwhile, Gosan 2006 showed the lowest PM_{10} and O_3 concentrations among the four campaigns but CO concentrations for all data and non-pollution days were the highest. The SO_2 concentration during Gosan 2008 was significantly lower than during the other campaigns, but its CO concentration is comparable to those in the other campaigns. BCMO 2009 had the lowest $PM_{2.5}$ and NO_2 (which is a subset of NO_y) concentrations, but its SO_2 concentration was the highest among all four campaigns except for Gosan 2007 pollution days. Therefore, no campaign had all six species low. These results indicate that the two sites were exposed to continental sources to some extent, even for the non-pollution period within each campaign.

The CO concentrations measured during these campaigns were mostly above 0.3 ppm, which is much greater than the values measured in nonurban tropospheric air, 0.07–0.2 ppm (Hobbs, 2000). Based on a 13-yr long-term measurement, Kaneyasu (2010) reported that continental influence was evident from late autumn to spring at Chichi-jima Island (27.07° N, 142.22° E), which lies in the northwestern Pacific 1800 km to the east of Chinese coastline. Even during the rest of the seasons, the black carbon concentration was still higher than at other background sites around the world, suggesting that the region still might not be completely free from continental influence. Compared to Chichi-jima Island, both islands in this study are located at a distance much closer to continental sources (<100 km from the Korean Peninsula and <500 km from China). Based on ship measurements during a cruise from a port on Jeju Island to Shanghai, Kim et al. (2009a) found that the instantaneous minimum N_{CN} in the East China Sea (1025 cm^{-3}) was still higher than the average N_{CN} measured at other background marine regions by a factor of two to five (Bates et al., 2002; Covert et al., 1996; Hoppel et al., 1990; Yum and Hudson, 2001). These previous studies also suggest that the two islands were under constant continental influence although the continental source could be different. Since the contribution of sea salt is known to be only minor for PM_{10} or $PM_{2.5}$ at the two islands (Lee et al., 2007; Kim et al., 2009b), high PM_{10} concentration can be considered to originate from continents.

3.2 Aerosol size distributions and CCN spectra

Averages and standard deviations of N_{CN}, N_{CCN}, the ratio between the two and geometric mean diameter measured during each campaign are shown in Table 1. Average CCN spectra for each campaign are shown in Fig. 5. N_{CN} from all four campaigns are comparable to that measured over the seas around the Korean Peninsula (Kim et al., 2009a), indicating that the two islands represent the maritime environment of the region. However, the same values are also higher than those from a pollution event at Gosan during 2001 (Kim et al., 2005), again indicating that the two islands are constantly under continental influence.

The average N_{CN} for BCMO 2009 was the highest among the four campaigns. This is consistent with the previous study by Kim et al. (2009a) who showed that N_{CN} over the Yellow Sea, where Baengnyeongdo lies, was higher than N_{CN} over the South Sea of Korea or the East China Sea,

Table 1. Average and standard deviation of N_{CN}, N_{CCN}, N_{CCN}/N_{CN}, and D_g for each campaign.

Location (Year)		Gosan (2006)	Gosan (2007)	Gosan (2008)	BCMO (2009)
Period		15 Aug–1 Sep	14 Apr–16 May	1 Aug–11 Oct	5 Aug–30 Aug
N_{CN} (cm^{-3})		4697±1823	4217±1514	3890±1808	5117±1880
N_{CCN} (cm^{-3})	1.0 % *S*	3290±1964	4074±1857[a]	2713±1271	4694±2567
	0.6 % *S*	2803±1545	3527±1718[a]	2076±989	4360±2297[b]
	0.2 % *S*	1550±659	1952±1286[a]	1043±646	3051±1310
N_{CCN}/N_{CN}	1.0 % *S*	0.77±0.16	0.96±0.15[a]	0.83±0.31	0.87±0.14
	0.6 % *S*	0.67±0.12	0.81±0.15[a]	0.60±0.25	0.82±0.16[b]
	0.2 % *S*	0.40±0.06	0.44±0.14[a]	0.29±0.15	0.59±0.20
D_g (nm)		98±25	94±14	81±24[c]	94±8[d]

[a] Only for the period 20 April–4 May.
[b] N_{CCN} and N_{CCN}/N_{CN} for 0.59 % *S*.
[c] The sample was dried prior to the measurement.
[d] Only for the period 26–28 August.

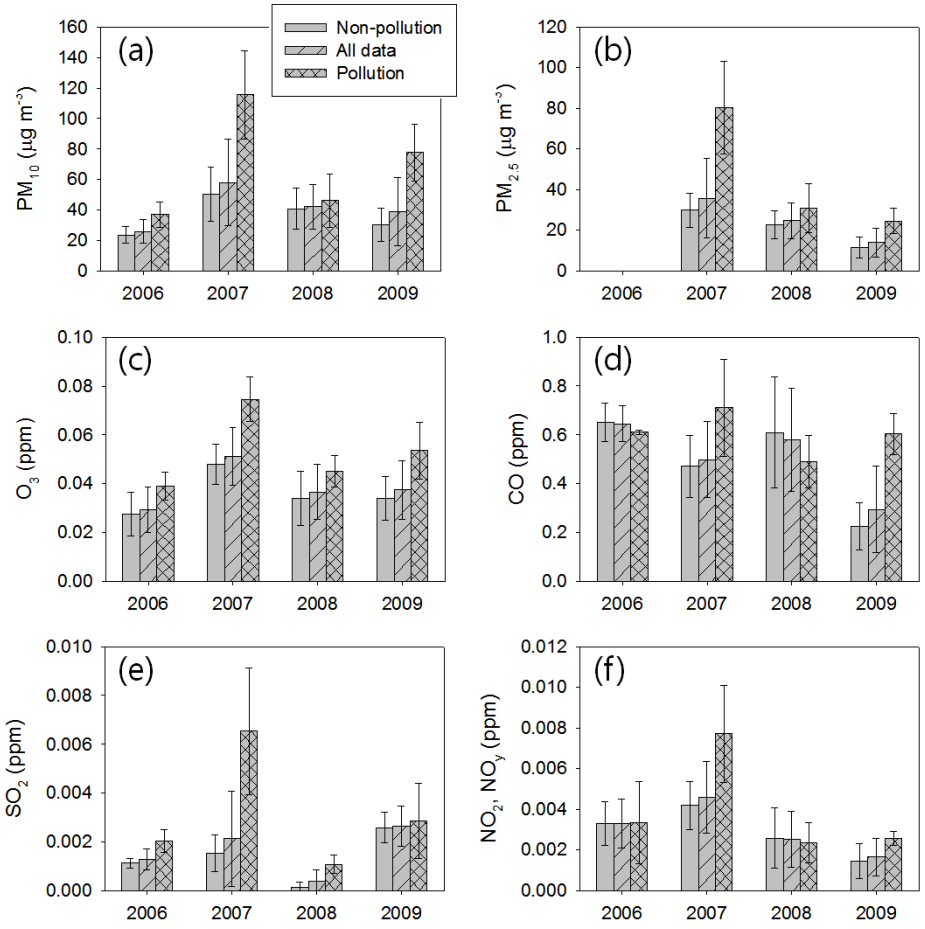

Fig. 4. Average concentrations of PM mass and of various gaseous species for each campaign. The error bars represent standard deviations of each measurement.

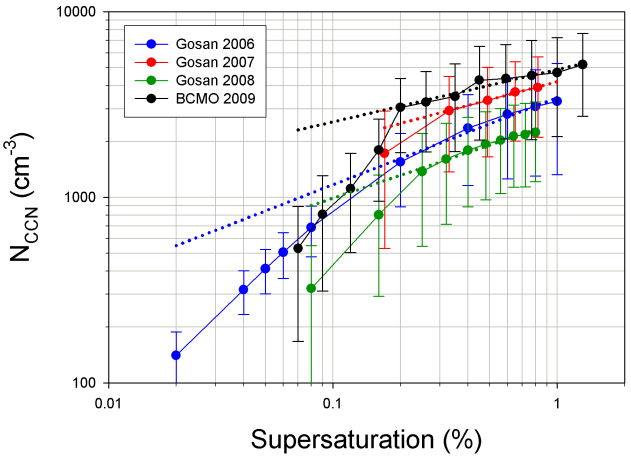

Fig. 5. Average CCN spectra (solid line) and power-law approximation for $S \geq 0.2\,\%$ (dotted line). The error bars represent standard deviations of N_{CCN}.

which surrounds Jeju Island. At BCMO, not only N_{CN} but also N_{CCN} was higher than at Gosan during the other campaigns for all measured $S \geq 0.1\,\%$ (Fig. 5). On the other hand, the lowest N_{CCN} was measured during Gosan 2008. The smaller D_g during Gosan 2008 than during the other campaigns is thought to be due to the effect of drying the SMPS sample air only during this campaign.

Time series of N_{CN}, N_{CCN} and D_g are shown in Fig. 6. During pollution days, N_{CN} and N_{CCN} tended to be at local maxima, but similarly high concentrations were also frequently found during non-pollution days. D_g values were generally larger during pollution days, mostly larger than 100 nm, implying that they had gone through aging processes accompanied by condensation since their emission.

There were a few short periods during Gosan 2006 and Gosan 2008 when the air mass apparently had no contact with land surface for five days before reaching the site. During such periods, N_{CN} and N_{CCN} were both much smaller than their averages. The data during such periods is provided as Supplement.

3.3 Hygroscopic growth factors below 90 % RH

For this section, growth factor (GF, defined as the ratio between the wet diameter and D_{dry}) values measured at various RH were converted to GF measured at 90 % RH (GF90) by the method illustrated in Swietlicki et al. (1999) to facilitate comparison between different campaigns. In short, the method assumes that the relationship between GF and RH for ambient particles is similar to that of ammonium sulfate droplets of the same wet diameter except that the Kelvin effect is considered. Converted GF90 values were then classified into four categories; "nearly hydrophobic" for GF90 smaller than 1.15, "less hygroscopic" for GF90 between 1.15 and 1.55, "more hygroscopic" for GF90 between 1.55 and 1.85 (similar to GF90 of ammonium sulfate) and "very hygroscopic" for GF90 larger than 1.85. This classification is similar to that by Massling et al. (2007) except that they denoted the class with the largest GF90 as "sea salt". Selected D_{dry} sizes varied in each campaign: 50, 100, 150 and 200 nm for Gosan 2006; 100, 150, 200 and 250 nm for Gosan 2007; 50, 100, 150, 200 and 250 nm for Gosan 2008; 53, 113, 163 and 225 nm for BCMO 2009.

The relative frequency of occurrence, or the cumulative number fraction, of each hygroscopicity class is shown for each campaign and each D_{dry} in Fig. 7. Average GF90 values, number fractions and number-weighted GF90 values for each size are listed in Table 2. As shown in Fig. 7, most of the GF90 values fell into either the less or more hygroscopic classes (1.15–1.85). Particles measured during Gosan 2007 and Gosan 2008 tended to show lower hygroscopicity compared to those measured during Gosan 2006 or BCMO 2009. Overall hygroscopicity was higher during BCMO 2009 than during the other campaigns. This is consistent with the above finding that N_{CCN}/N_{CN} for $S \leq 0.6\,\%$ and SO_2 concentrations were the largest during BCMO 2009 of the four campaigns.

As for the mixing state, 82 %, 97 %, 99 % and 98 % of HTDMA samples measured during Gosan 2006, Gosan 2007, Gosan 2008 and BCMO 2009, respectively, had only a single GF mode, suggesting that the aerosols were mostly internally mixed or that all particles of each size range had very similar hygroscopicities. During Gosan 2006, Gosan 2007 and Gosan 2008, "nearly hydrophobic" particles were highly likely to be found (more than four out of five) when there was more than one GF mode. For Gosan 2008, however, more than half of "nearly hydrophobic" particles were found with a single GF mode. During BCMO 2009, "nearly hydrophobic" particles were found only in a small fraction. Even when the sample had more than one GF mode, it consisted only of "less hygroscopic" and "more hygroscopic" modes, suggesting that these particles had gone through aging processes perhaps due to high sulfur concentrations in the region. GF90 distributions during pollution days were similar to those of non-pollution days, suggesting that continental sources were constantly affecting the sites even on the days classified as non-pollution days.

When compared to the previous HTDMA measurement during ACE-Asia (Massling et al., 2007), the values during Gosan 2006 in Table 2 are similar to the results for pollution from Shanghai and a dust period measured onboard NOAA Research Vessel *Ronald H. Brown* at a location about 400–600 km east of Gosan, where a minor but significant portion was "nearly hydrophobic" and the most abundant class was "more hygroscopic". Gosan 2007 and Gosan 2008 were unique in that the "less hygroscopic" class was dominant. BCMO 2009 is similar to the case when the pollution had passed over Korea and Japan before reaching R/V *Ronald H. Brown*, although the majority of air masses were from northeastern China during BCMO 2009.

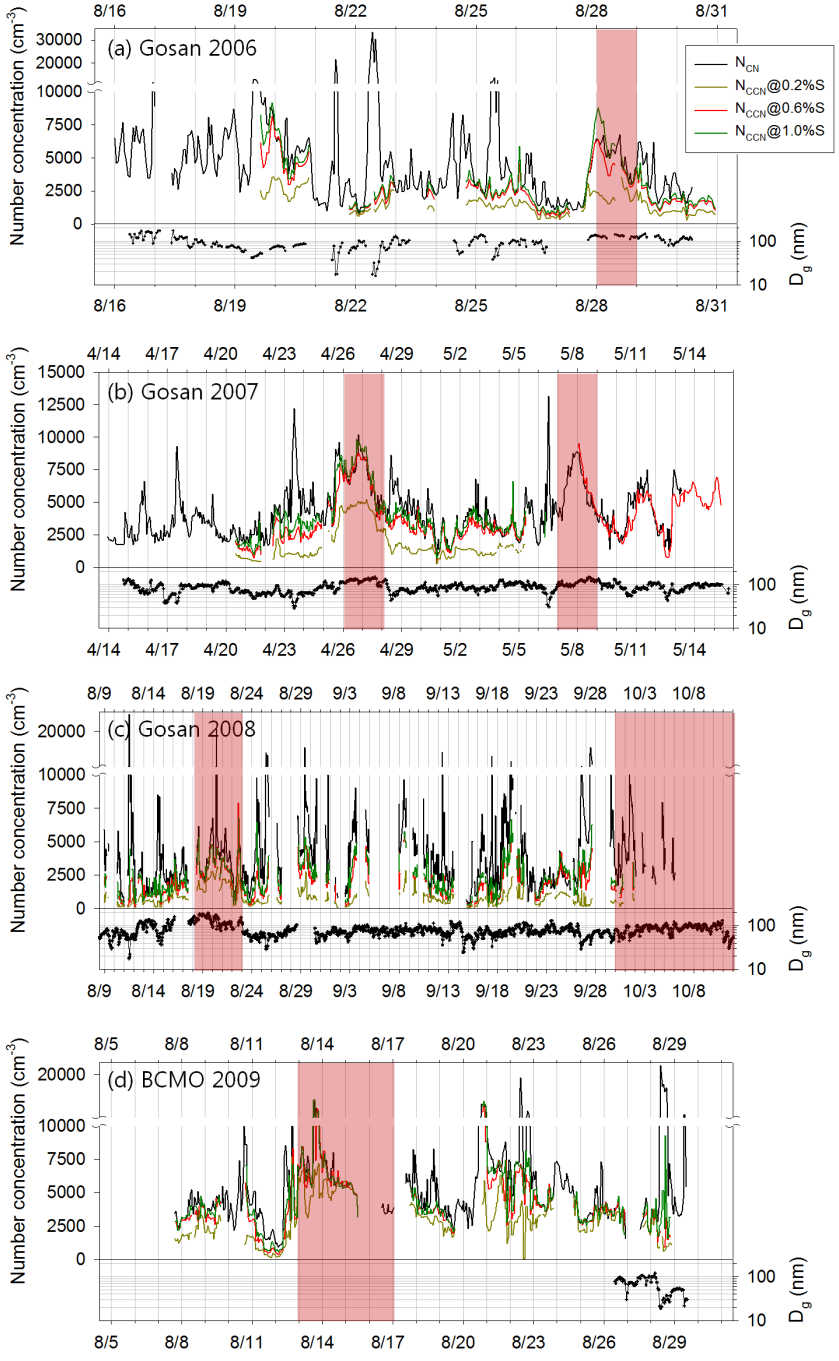

Fig. 6. Time plots of measured N_{CN}, N_{CCN} and D_g for each campaign. Pollution periods are shaded in red.

The GF90 values in this study were mostly in the range of 1.4–1.7 for all sizes, similar to or even higher than the most hygroscopic modes measured in Beijing during summer 2004 and winter 2005 (Massling et al., 2009), which is located at the dominant upwind region of the measurement sites. As with the previous discussion, this is another indication that aerosols reaching the two islands have gone through chemical aging during transport.

3.4 Critical supersaturation (S_c)

Time variations of S_c measured during Gosan 2008 and BCMO 2009 are plotted in Fig. 8. Note that the measurement period was much longer during Gosan 2008. As shown in Fig. 8a, some S_c data were missing for 50 nm particles during Gosan 2008 because the full shape of the sigmoid curve (e.g. Fig. 3) could not be constructed due to a limited S range.

Table 2. Average and standard deviation of GF90 and cumulative number fraction (NF) of each hygroscopicity class; class 1, 2, 3 and 4 corresponds to "nearly hydrophobic", "less hygroscopic", "more hygroscopic" and "very hygroscopic", respectively.

Period	D_{dry} (nm)	GF90_1	GF90_2	GF90_3	GF90_4	NF_1	NF_2	NF_3	NF_4	Number weighted GF90
Gosan	50	1.00±0.06	1.40±0.11	1.59±0.03	–	0.29±0.31	0.61±0.32	0.10±0.19	–	1.30
2006	100	1.05±0.04	1.50±0.05	1.66±0.06	–	0.22±0.23	0.33±0.38	0.45±0.33	–	1.47
	150	1.04±0.03	1.52±0.02	1.71±0.09	1.87±0.03	0.14±0.22	0.22±0.37	0.59±0.40	0.05±0.16	1.58
	200	1.02±0.02	1.51±0.03	1.67±0.08	1.87±0.02	0.10±0.15	0.15±0.21	0.66±0.30	0.09±0.16	1.60
	250	–	–	–	–	–	–	–	–	–
Gosan	50	–	–	–	–	–	–	–	–	–
2007	100	1.07±0.04	1.48±0.06	1.58±0.03	–	0.05±0.08	0.66±0.23	0.30±0.25	–	1.50
	150	1.05±0.03	1.48±0.05	1.57±0.01	–	0.05±0.11	0.70±0.26	0.25±0.24	–	1.48
	200	1.04±0.05	1.47±0.04	1.57±0.01	2.17*	0.03±0.10	0.67±0.25	0.30±0.25	0.04*	1.57
	250	1.08±0.04	1.48±0.05	1.58±0.02	–	0.03±0.06	0.66±0.25	0.32±0.23	–	1.51
Gosan	50	1.07±0.04	1.32±0.07	–	–	0.22±0.25	0.78±0.25	–	–	1.27
2008	100	1.08±0.05	1.32±0.06	–	–	0.14±0.25	0.86±0.25	–	–	1.29
	150	1.06±0.04	1.41±0.06	1.57±0.01	–	0.09±0.19	0.87±0.22	0.05±0.14	–	1.40
	200	1.08±0.02	1.43±0.05	1.58±0.02	–	0.04±0.10	0.88±0.23	0.09±0.21	–	1.44
	250	1.06±0.02	1.44±0.04	1.57±0.01	–	0.03±0.10	0.85±0.25	0.12±0.24	–	1.44
BCMO	53	1.07±0.03	1.47±0.08	1.65±0.04	–	0.04±0.08	0.24±0.31	0.72±0.31	–	1.58
2009	113	0.99±0.02	1.50±0.04	1.62±0.04	–	0.01±0.03	0.25±0.32	0.74±0.32	–	1.58
	163	1.06±0.02	1.42±0.16	1.74±0.06	1.87±0.03	0.01±0.04	0.04±0.11	0.87±0.20	0.09±0.19	1.75
	225	1.08±0.07	1.51±0.04	1.68±0.06	1.92±0.05	0.04±0.10	0.07±0.15	0.85±0.21	0.04±0.13	1.65

* Only a single measurement was available.

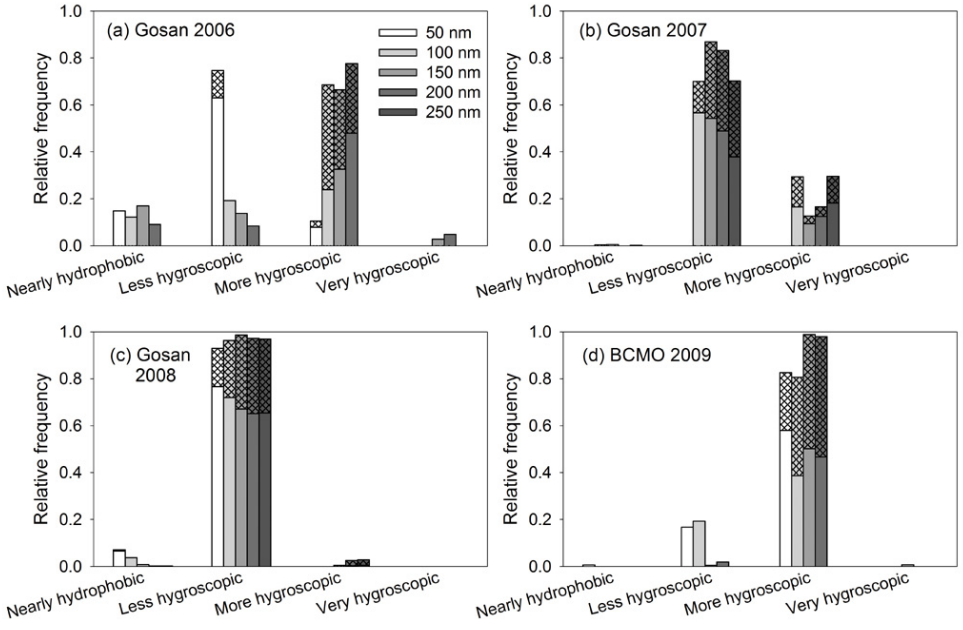

Fig. 7. Relative frequency of occurrence of each hygroscopicity class for each dry diameter during each campaign. Meshed part indicates the portion for pollution days. For BCMO 2009, dry diameters are 53, 113, 163, 225 nm.

During BCMO 2009, S_c values for the two monodisperse dry particle sizes were relatively larger for the periods before 13 August than after 13 August. This distinction between these periods was also found in the $PM_{2.5}$ and SO_2 data. According to 72 h back trajectory analyses, all the air masses that reached BCMO before 13 August passed over the Korean Peninsula whereas the air masses after 13 August passed mostly over northeastern China. Kim et al. (2009b) reported

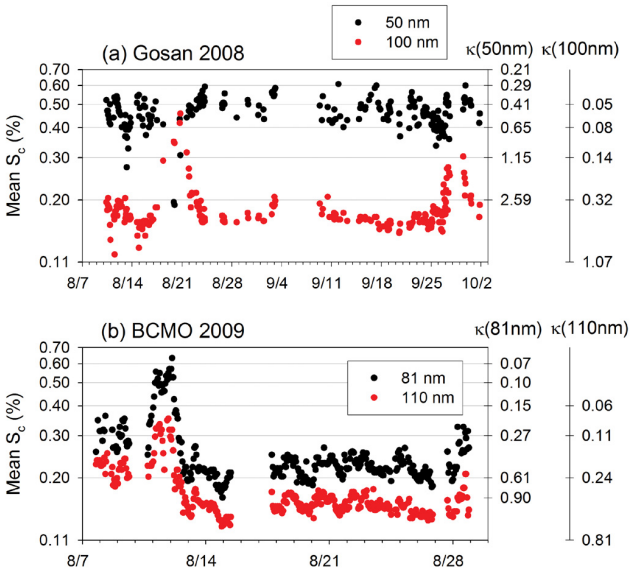

Fig. 8. Time plots of S_c during Gosan 2008 (top) and BCMO 2009 (bottom). The κ values for corresponding S_c values for each dry diameter are shown on the right.

a clear distinction in inorganic compounds of submicron particles measured by an Aerodyne aerosol mass spectrometer at BCMO between the back trajectories that passed over the Korean Peninsula and those that passed over northeastern China, i.e. Shandong Peninsula or Bohai Bay. Nitrate was abundant for the former while sulfate was abundant for the latter. The difference in S_c between the two periods cannot be attributed to the difference in nitrate and sulfate concentrations because nitrate is as hygroscopic as sulfate (Brechtel and Kreidenweis, 2000) and because the abundant amount of organics for both back trajectories also need to be considered. Different particle compositions, however, reveal that aerosol sources were different between the Korean Peninsula and northeastern China. From a field study during spring 2008, Mochida et al. (2010) reported that aerosols reaching Cape Hedo from China and the Pacific had higher GF and lower D_{p_act}, compared to those from Korea and Japan, which may be supportive of our suggestion that aerosols from Chinese sources tend to have lower S_c compared to those from Korean/Japanese sources. On the other hand, no such clear distinction of S_c was found during Gosan 2008.

In Table 3 CCN activity parameters such as D_{p_act}, S_c or GF90 reported in previous studies in East Asia are compared with those measured in this study along with the corresponding values of κ (Petters and Kreidenweis, 2007). The average S_c for 50 nm during Gosan 2008 is not shown because S_c higher than 0.61 % could not be estimated due to the limited S range as explained above. These samples were a non-negligible portion. Overall, the κ values measured during BCMO 2009 are higher than those measured during Gosan 2008, which is in accordance with N_{CCN}/N_{CN} and HTDMA measurements.

Although no previous studies have measured S_c in East Asia, several studies have characterized CCN activity by measuring the D_{p_act} with a similar instrument setup to that in Fig. 2. Those studies varied D_{dry} and set S fixed ("D_{dry} scan") while in this study instead S was varied ("S scan") and D_{dry} was fixed. Under the assumption that aerosols are all internally mixed and that aerosols have homogeneous hygroscopicity across the whole submicron size range, CCN activity measured from both settings should agree with each other.

Su et al. (2010) quantified the difference between the two methods if aerosol hygroscopicity varies with particle size. They considered a case when κ varied with size as $\kappa = 0.2 \times \left(\frac{D_{dry}}{20\,nm}\right)^{0.4}$ that causes much larger variations compared to the ones measured in this study. They concluded that the difference between the two methods due to size-dependent hygroscopicity should be relatively minor compared to the instrumental uncertainties. Since the aerosols were mostly internally mixed except for Gosan 2006, as discussed above, it would not be too misleading to compare S_c in this study by "S scan" to the activation diameter obtained in previous studies by "D_{dry} scan" when both measured quantities are converted to κ.

As shown in Table 3, the values of κ obtained at Gosan by HTDMA show a decreasing trend since 2005, and the decrease is more significant for smaller D_{dry}. Seasonal variation is not sufficient to explain such a decreasing trend, since the 2005 campaign and Gosan 2007 were both carried out during late spring. Moreover, the measurement days of Gosan 2006 are covered by those of Gosan 2008. Such a trend is also found for DMA-CCN measurements: the κ values measured during 2005 are larger than those measured during Gosan 2008. Although the two DMA-CCN instruments were based on different concepts i.e. "D_{dry} scan" for 2005 and "S scan" for 2008, the difference between the two sets of κ values are too large to be attributed to a methodological difference as discussed above. The reason behind such decreasing trend is left unknown.

It is also worth noting that during Gosan 2006 and Gosan 2008, HTMDA measurement found slightly increasing κ with increasing size, but such size dependence was insignificant during Gosan 2007. Kuwata et al. (2008) also found a similar size dependency at Gosan, although their κ value was generally higher. In contrast, DMA-CCN measurements during Gosan 2008 found smaller κ for the larger size, 100 nm, when S_c values for both sizes were simultaneously available. Such opposite size dependence was independent of the selection of a Köhler model provided in Rose et al. (2008). When the air mass was coming from northeast China near Yufa, about 50 km south of Beijing, it usually took a day or two for the air mass to reach BCMO. If the results from Wiedensohler et al. (2009) are presumed to be representative of northeast China during August 2009, one can say that hygroscopicity increased as the aerosol advected from

Table 3. Comparison of κ values obtained from various hygroscopicity studies in East Asia. In BCMO 2009 and Massling et al. (2007), the results were classified by air mass back trajectories (nC: northern China, KP: Korean Peninsula, KJ: Korea/Japan, Sd: Shanghai/dust).

Location (Period)	Method	D_{p_act} (nm), S_c(% S), GF	Corresponding κ	Reference
Gosan, south of Korean Peninsula (Mar–Apr 2005)	DMA-CCN	136±17 nm (0.097 % S)[a] 71±6 nm (0.27 % S)[a] 44±3 nm (0.58 % S)[a] 31±3 nm (0.97 % S)[a]	0.61±0.17 (0.097 % S)[a] 0.55±0.12 (0.27 % S)[a] 0.50±0.09 (0.58 % S)[a] 0.55±0.13 (0.97 % S)[a]	Kuwata et al. (2008)
Gosan, south of Korean Peninsula (Aug 2006)	HTDMA	1.33± 0.15 (50 nm) 1.49±0.14 (100 nm) 1.55±0.19 (150 nm) 1.61±0.14 (200 nm)	0.28±0.15 (50 nm) 0.41±0.14 (100 nm) 0.49±0.18 (150 nm) 0.53±0.16 (200 nm)	This study
Gosan, south of Korean Peninsula (Apr–May 2007)	HTDMA	1.48±0.07 (100 nm) 1.48±0.05 (150 nm) 1.48±0.05 (200 nm) 1.49±0.06 (250 nm)	0.25±0.04 (100 nm) 0.23±0.03 (150 nm) 0.23±0.04 (200 nm) 0.23±0.05 (250 nm)	This study
Gosan, south of Korean Peninsula (Aug–Oct 2008)	HTDMA DMA-CCN	1.30±0.08 (50 nm) 1.31±0.06 (100 nm) 1.41±0.06 (150 nm) 1.43±0.06 (200 nm) 1.45±0.05 (250 nm) 0.19±0.02 % S (100 nm)	0.17±0.05 (50 nm) 0.16±0.04 (100 nm) 0.21±0.04 (150 nm) 0.22±0.05 (200 nm) 0.23±0.04 (250 nm) 0.40±0.07 (100 nm)	This study This study
BCMO, west of Korean Peninsula (Aug., 2009)	HTDMA[b] DMA-CCN 	1.61±0.06 (53 nm, nC) 1.60±0.06 (113 nm, nC) 1.74±0.06 (163 nm, nC) 1.67±0.06 (225 nm, nC) 0.33±0.08 % S (81 nm, KP) 0.22±0.04 % S (110 nm, KP) 0.22±0.02 % S (81 nm, nC) 0.15±0.01 % S (110 nm, nC)	0.42±0.05(53 nm, nC) 0.36±0.04(113 nm, nC) 0.48±0.05(163 nm, nC) 0.41±0.04(225 nm, nC) 0.28±0.12 (81 nm, KP) 0.35±0.09 (110 nm, KP) 0.52±0.07 (81 nm, nC) 0.43±0.05 (110 nm, nC)	This study This study
East Sea (Apr., 2001)	HTDMA	1.55 (50 nm, KJ)[c] 1.69 (150 nm, KJ)[c] 1.67 (250 nm, KJ)[c] 1.64 (350 nm, KJ)[c] 1.62 (50 nm, Sd)[c] 1.68 (150 nm, Sd)[c] 1.61 (250 nm, Sd)[c] 1.54 (350 nm, Sd)[c]	0.35 (50 nm, KJ)[c] 0.44 (150 nm, KJ)[c] 0.42 (250 nm, KJ)[c] 0.39 (350 nm, KJ)[c] 0.41 (50 nm, Sd)[c] 0.43 (150 nm, Sd)[c] 0.36 (250 nm, Sd)[c] 0.30 (350 nm, Sd)[c]	Massling et al. (2007)
Cape Hedo, Japan (Apr 2007)	HTDMA DMA-CCN 	1.39±0.06 (49 nm)[d] 1.43±0.05 (71 nm)[d] 1.47±0.04 (125 nm)[d] 130±3 nm (0.10 % S) 78±5 nm (0.25 % S) 54±5 nm (0.44 % S)	0.37±0.07 (49 nm)[d] 0.39±0.05 (71 nm)[d] 0.42±0.04 (125 nm)[d] 0.69 (0.10 % S)[e] 0.51 (0.25 % S)[e] 0.50 (0.44 % S)[e]	Mochida et al. (2010) Mochida et al. (2010)
Beijing, northeastern China (Jun–Jul 2004)	HTDMA	1.23 (50 nm)[c] 1.37 (150 nm)[c] 1.42 (250 nm)[c] 1.45 (350 nm)[c]	0.11 (50 nm)[c] 0.18 (150 nm)[c] 0.21 (250 nm)[c] 0.23 (350 nm)[c]	Massling et al. (2009)
Beijing, northeastern China (Jan–Feb 2005)	HTDMA	1.27 (50 nm)[c] 1.36 (150 nm)[c] 1.30 (250 nm)[c] 1.28 (350 nm)[c]	0.14 (50 nm)[c] 0.18 (150 nm)[c] 0.14 (250 nm)[c] 0.12 (350 nm)[c]	Massling et al. (2009)
Yufa, northeastern China (23 August 2006)	DMA-CCN	190±3 nm (0.07 % S) 84±5 nm (0.26 % S) 62±6 nm (0.46 % S) 45±7 nm (0.86 % S)	0.45 (0.07 % S)[f] 0.38 (0.26 % S)[f] 0.30 (0.46 % S)[f] 0.22 (0.86 % S)[f]	Wiedensohler et al. (2009)

[a] Taken from Table 2 of Kuwata et al. (2008). [b] No HTDMA results were available for KP back trajectories. [c] Average GF were calculated from number-weight averaging of the GF values measured at 90 % RH in each hygroscopicity class given in the appendix tables in each study. Corresponding κ values were then calculated from the average GF90 with T=15°C. [d] GF values were measured at 85 % RH. Taken from Table 2 of Mochida et al. (2010). [e] Calculated from average D_{p_act} in Table 1 of Mochida et al. (2010) with T=15°C. [f] Calculated from average D_{p_act} in Fig. 12 of Wiedensohler et al. (2009) with $T = 15\,^{\circ}$C.

northeast China to BCMO, perhaps due to aging processes during the transport.

4 Discussion

4.1 CCN spectrum parameterization

The power law approximation ($N_{CCN} = C \times S^k$) to CCN spectra is a convenient tool to model CCN spectra (Pruppacher and Klett, 1997 and references therein; Hudson et al., 1998; Hudson and Yum, 2001; Yum and Hudson, 2001). In Fig. 5 such approximations are shown by dotted lines for each campaign with the corresponding color. The approximation is based on N_{CCN} for $S \geq 0.2\,\%$ but the lines are extrapolated to the lowest S. The range of $S \geq 0.2\,\%$ was selected for two reasons; the spectra show somewhat exponential behavior in this range (suggested by the linearity of the spectra in Fig. 5) and several field studies that compared the measured cumulative CCN spectrum below cloud base with the measured cloud droplet concentrations in clouds suggested the effective supersaturation in clouds to be 0.2 % or higher for stratocumulus and stratus clouds (Yum et al., 1998; Yum and Hudson 2002; Hudson et al., 2010). The parameters (C, k) for power law approximation for $S \geq 0.2\,\%$ are shown in Table 4. However, it should be noted that the power law approximation usually holds only for a limited range of S, as various previous studies have emphasized (Khain et al., 2000 and references therein). Dusek et al. (2003) have also argued that using a traditional power function is not backed by any physical reason and that its application should be confined only to clean marine CCN spectra. As can be seen in Fig. 5, although the power law approximation had high r^2 values for the linear regression between the measured and parameterized N_{CCN} values for $S \geq 0.2\,\%$ (0.98, 0.96, 0.89 and 0.94 for 2006, 2007, 2008 and 2009 campaign, respectively), they all significantly overestimated N_{CCN} at $S < 0.2\,\%$ and the magnitude of overestimation increased with decreasing S. The N_{CCN} predicted by the power law approximation at 0.02 % S for Gosan 2006, and at 0.07 % S for Gosan 2008 and BCMO 2009 were 3.9, 3.2 and 4.3 times larger than the measured N_{CCN} at the corresponding S, respectively. For that reason, the parameters C and k that can be obtained by linearly extending the CCN spectra only for $S \leq 0.2\,\%$ range to the lowest S for each campaign in Fig. 5 are also shown in Table 4.

4.2 Comparison of hygroscopic growth and CCN activation

Figure 9 compares the estimated κ values from the S_c measurements of monodisperse particles during Gosan 2008 (50 and 100 nm) and BCMO 2009 (110 nm) with those from the simultaneous HTDMA measurements for the same (for Gosan 2008) or very similar (113 nm for BCMO 2009) diameters. The κ (GF) was calculated from the actual GF and

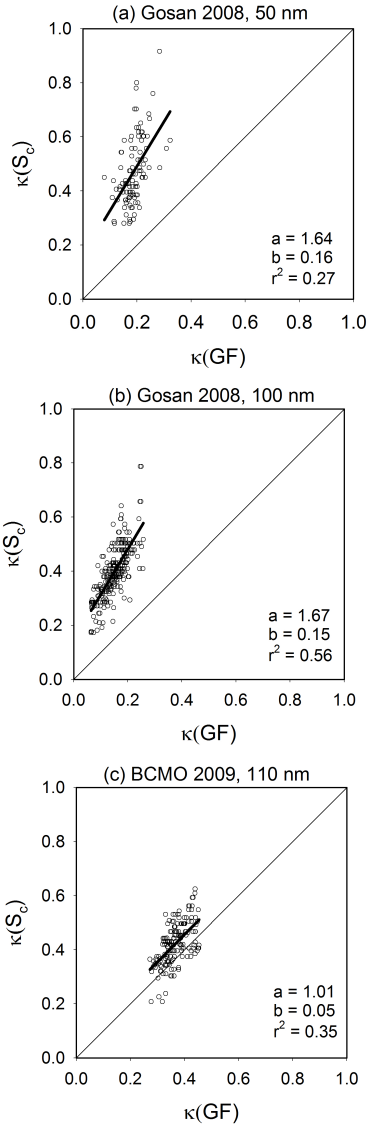

Fig. 9. Comparison of the estimated κ values from GF and S_c measurements for 50 and 100 nm D_{dry} during Gosan 2008 and for 110 nm D_{dry} during BCMO 2009. The linear regression line ($y = ax + b$, thick solid line) and the coefficient of determination (r^2) are also shown.

RH, not GF90. Most of the κ (S_c) were larger than the simultaneously measured κ (GF) although the difference between the two was much smaller for BCMO 2009. For each case the regression slopes were 1.64, 1.67 and 1.01, respectively, for the three plots in Fig. 9 and their r^2 values were all below 0.6.

The differences between κ (S_c) and κ (GF) found in most of the samples are beyond expected instrumentation uncertainty. Petters and Kreidenweis (2008) showed that the presence of sparingly soluble organics within the particles which dissolve only at supersaturated conditions could contribute to

Table 4. Parameters C and k of the CCN spectra power law approximations for two S ranges in each campaign.

Period	$S \geq 0.2\,\%$	$S \leq 0.2\,\%$
Gosan 2006	($3438\,cm^{-3}$, 0.47)	($8977\,cm^{-3}$, 1.04)
Gosan 2007	($4194\,cm^{-3}$, 0.32)	N/A
Gosan 2008	($2533\,cm^{-3}$, 0.41)	($9012\,cm^{-3}$, 1.32)
BCMO 2009	($4879\,cm^{-3}$, 0.28)	($36304\,cm^{-3}$, 1.60)

higher κ (S_c). Detailed chemical analysis of aerosols is out of the scope of this study but it was reported that a significant organic fraction was consistently found at the submicron size range both at Gosan (Lee et al., 2007) and BCMO (Kim et al., 2009b), which may have partially contributed to such an effect. However, as discussed later, N_{CCN} prediction based on κ (S_c) resulted in significantly larger over-prediction compared to the prediction based on κ (GF). Such a result implies that sparingly soluble organics alone cannot explain the difference between the two because if that were the case, κ (S_c) should result in better prediction than κ (GF).

4.3 CCN closure study

Since CCN activity depends mostly on D_{dry}, and hygroscopicity, N_{CCN} at a given S can be calculated from the aerosol dry size distribution and hygroscopicity. Recently, Andreae and Rosenfeld (2008; hereafter AR08) put together various hygroscopicity measurements around the world and suggested that $\kappa = 0.3 \pm 0.1$could be used for global continental aged aerosols in numerical models targeted for understanding aerosol indirect effects on climate. A pioneering study to investigate global distribution of κ using global numerical simulation also reached a similar result, 0.27 ± 0.21, for continental aerosol (Pringle et al., 2010). As shown in previous sections, it is certain that most of the aerosols measured in this study have continental origin and that they have gone through aging processes during transport. Therefore, the data presented in this work will provide a suitable test bed for hygroscopicity values suggested by AR08. The fact that hygroscopicity was measured with high temporal resolution will also enhance the understanding of how size and temporal variation affect N_{CCN}.

In order to do so, measured N_{CCN} were compared with the values predicted by several different methods where hygroscopicity was uniquely assigned to individual size bins for each method as shown in Table 5. Since all of these methods require dry size distribution data, the CCN closure was performed only for the data obtained during Gosan 2008 because the size distribution was not measured at dried state during the other campaigns. All aerosols were assumed to be internally mixed, since 99 % of the samples were internally mixed during Gosan 2008 as shown in the previous section. With the assumption of all particles internally mixed in the same proportions for all sizes, a κ value is assigned to each size bin in dry size distribution data and compared with the minimum κ required for the particles in that size bin to be activated as CCN at a given S. If the assigned κ for that size bin is larger than the minimum κ for activation at the given S, then all of the particles in that size bin are counted as CCN. After carrying out such comparisons and counting cumulatively the concentrations for every size bin that meets the condition, the predicted N_{CCN} is obtained. One thing to note is that κ can vary within each size bin because of composition variations among particles in the same size bin but this was not taken into account in our study.

For the first method, denoted as "Method 1-GF", measured GF was first converted to corresponding κ (GF, D_{dry}) and then was averaged hourly for every size bin. Then the 1-h averaged κ (GF, D_{dry}) was linearly interpolated over the size bins with log-uniform intervals. For the size bins lying outside of the hygroscopicity measurement, the measured κ value of the nearest D_{dry} was used. An example of such a procedure is shown in Fig. 10. The solid line indicates the assigned κ value for each size bin interpolated from κ (GF, D_{dry}). The dashed line denotes the minimum κ required for particles in each size bin to be activated as CCN at 0.6 % S. The simultaneously measured dry aerosol size distribution is also shown. Only the particles in the size bins where the assigned κ values are greater than the minimum κ (colored in grey) are assumed to be activated as CCN and they are cumulatively counted for predicting N_{CCN} at 0.6 % S.

The second method is similar to the first one except that it ignores the size-resolving information. This is to see the effect of size-resolved hygroscopicity on N_{CCN}. The average κ (GF) from the two smallest diameters for each hour was applied to all size bins measured during that hour. The reason for choosing the two smallest diameters for representing the hygroscopicity of the whole submicron aerosol becomes obvious in Fig. 11. Compared with the threshold κ values for activation for S between 0.2–1.0 % (denoted by colored squares), most particles with D_{dry} larger than 150 nm can be activated for $S \geq 0.2\,\%$ regardless of the choice of any κ within the measured range. On the other hand, the threshold κ for activation increases sharply with D_{dry} smaller than 100 nm and CCN activity becomes sensitive to κ. This method is denoted as "Method 2-GF (small)".

A similar method of using a single κ for all sizes can be done with the average κ for the two largest diameters (200 and 250 nm), where aerosol mass faction is large. Various aerosol chemistry measurements like filter-based measurement or mass spectrometry rely on aerosol mass concentration. This method is denoted as "Method 2-GF (large)" and can be considered as a proxy for using such chemistry data for N_{CCN} closure. Another way is to use the κ values deduced from S_c measurement. The S_c value for 50 nm was available only for less than half of Gosan 2008. Therefore the κ deduced from S_c for 100 nm was used as the single

Table 5. Average and standard deviation of relative deviation, defined as $|N_{CCN\_pred} - N_{CCN\_meas}|/N_{CCN\_meas}$, for different CCN closure methods using the GF and Sc data. The values are given in units of percent and the word in the parentheses indicates whether the closure results are dominated by underprediction (under-), overprediction (over-) or balanced.

Method	Description	0.2 % S	0.6 % S	1.0 % S
1-GF	Time varying and size segregated κ(GF) are used	28±20 (under-)	25±52 (balanced)	19±15 (balanced)
2.GF (small)	Time varying average κ(GF) for 50 and 100 nm are used for all sizes.	32±17 (under-)	25±51 (balanced)	19±14 (balanced)
2-GF (large)	Time varying average κ(GF) for 200 and 250 nm are used for all sizes.	25±24 (under-)	31±57 (over-)	22±17 (balanced)
3-GF	Size segregated but temporally averaged κ(GF) are used for all time.	28±38 (under-)	26±39 (over-)	23±29 (balanced)
2-S_c	Time varying $\kappa(S_c)$ for 100 nm is used for all sizes.	38±42 (over-)	42±57 (over-)	30±37 (over-)
3-S_c	Temporally averaged $\kappa(S_c)$ for 100 nm is used for all sizes and time.	50±68 (over-)	47±61 (over-)	34±42 (over-)
AR08	Fixed κ value of 0.3 is used for all sizes and time.	30±51 (over-)	41±56 (over-)	28±35 (over-)
AR08-refined	Fixed κ value of 0.17 and 0.3 is used for sizes below and above 100 nm, respectively, for all time.	28±38 (under-)	26±39 (over-)	23±29 (balanced)

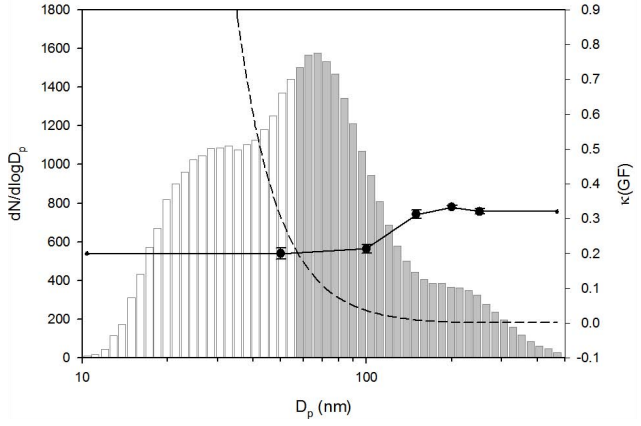

Fig. 10. An example of predicting N_{CCN} at 0.6 % S by combining measured κ(GF) (line with circle symbols) with the size distribution. The dashed line denotes the minimum κ required for each size bin to be activated as CCN at 0.6 % S. Only the grey vertical boxes are summed up to obtain the predicted N_{CCN} based on the GF measurement. The error bars represent standard deviations of κ(GF).

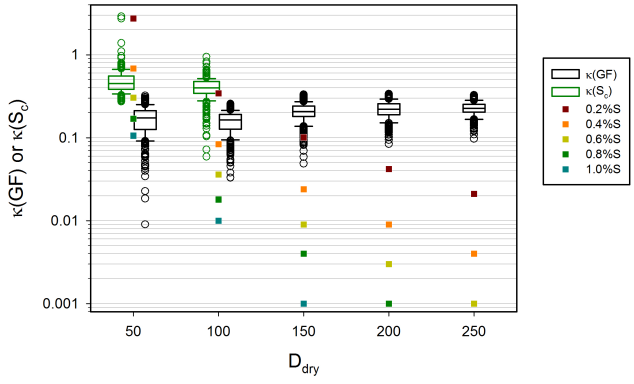

Fig. 11. Hygroscopicity parameter κ for each D_{dry} during Gosan 2008. κ(GF) and $\kappa(S_c)$ are calculated from measured GF and S_c values, respectively. Threshold κ values for CCN activation under selected S are shown as colored squares. The horizontal bar within the box indicates the median value and the upper and lower ends of the box represent 75 and 25 percentiles, respectively. The upper and lower whiskers outside the box represent 90 and 10 percentiles, respectively. Data outside of the 10–90 percentile range are considered outliers and each data point is marked with an open circle.

κ for N_{CCN} closure and this method is denoted as "Method 2-S_c".

In "Method 3-GF", the campaign-averaged κ values deduced from the GF measurements at the five different diameters shown in Table 3 are used to assign κ to each size bin as explained in Fig. 10. Here the difference is that these values are applied to all size distribution data measured during the campaign, neglecting temporal variation of κ. "Method 3-S_c" is similar: the campaign-averaged κ value of 0.4 deduced from S_c for 100 nm (Table 3) is assigned for all size distribution data. Therefore, by comparing "Method 3" to

"Method 1", the effect of temporal variation of hygroscopicity can be found.

For the last method, "Method AR08", κ was set to 0.3 as suggested by AR08 and only the temporal variation of the size distribution was taken into account.

The results of all closures are illustrated in Fig. 12 and the quantitative comparison of the results is made in Table 5 where the averages and standard deviations of relative deviation, are shown, which is defined as the ratio of the absolute difference between predicted and measured N_{CCN} to measured N_{CCN}. Also shown in the table is the short description for each method and whether the closure results are dominated by under-prediction, over-prediction or balanced. The closure results only for the pollution days showed no noticeable difference compared to those for non-pollution days.

For all methods, the smallest average relative deviation was found for 1.0 % S indicating that the importance of assigned κ information diminishes as S increases because most particles would be activated regardless of their κ value when S is high. The largest standard deviation of relative deviation was found for 0.6 % S, which means that accuracy of N_{CCN} prediction significantly varied from case to case for this S. For 0.6 % S, measured κ was near the threshold value for 50 and 100 nm (Fig. 11) and therefore predicted N_{CCN} was most sensitive to the assigned κ.

Now we compare the different methods. It is found that the average κ for the two largest diameters (200 and 250 nm) poorly represents aerosol hygroscopicity for higher S: the relative deviation of "Method 2-GF (large)" for 0.6 % S is not only larger than "Method 2-GF (small)" but also larger than "Method 3-GF" where temporal variation of hygroscopicity was completely ignored. This suggests that chemistry information of aerosols smaller than 100 nm diameter cannot be substituted by bulk measurements that mostly represent aerosols of larger diameters than 100 nm. Kammermann et al. (2010) drew a similar conclusion from their GF measurements, i.e. that assigning the hygroscopicity measured for aerosols of diameter 180–200 nm to all sizes resulted in poor CCN closure. Ervens et al. (2010) also made a similar suggestion that identifying hydrophobic organics of diameter $\sim$100 nm is important for CCN closure.

Because the relative deviation of Method 3-GF is comparable to that of Method 1-GF, it can be said that the effect of temporal variation of hygroscopicity had a minor effect on CCN closure. However, it should be noted that Gosan 2008 lasted only 2 months and temporal variations of hygroscopicity may be important when one needs to deal with longer periods.

The methods using S_c data (Method 2-S_c, Method 3-S_c) show larger relative deviations than the methods using GF data. Even the method using the constant κ (Method AR08) shows smaller relative deviations. There were many more over-predicted than under-predicted values for these two methods (Fig. 12e and f), which is in accordance with Fig. 9b where κ (S_c) was larger than κ (GF) and mostly larger than $\kappa = 0.3$.

The comparison between the CCN prediction by Method 1 and that by Method AR08 is shown in Fig. 12h. Assuming the constant κ of 0.3 resulted in over-prediction by 64 ± 58 %, 33 ± 27 % and 14 ± 14 % for 0.2, 0.6 and 1.0 % S, respectively, compared to Method 1. The degree of disagreement between the two methods is larger for lower S. This implies that using the N_{CCN} predicted by AR08 as input to a model that calculates cloud droplet concentration (e.g. Cubison et al., 2008) could result in higher cloud droplet concentration than using the N_{CCN} predicted by Method 1. Eventually this could result in overestimation of droplet concentrations in cloud models and this would impact cloud properties.

Figure 13 illustrates detailed feature of the over-prediction when using Method AR08. Here relative deviations from Method AR08 are compared to those from Method 1-GF as a function of N_{CCN} at 0.6 % S. The relative deviations of Method AR08 tend to increase as N_{CCN} decreases from the largest (3787–7203 cm^{-3}) to the smallest bin (289–550 cm^{-3}) (Fig. 13a). Figure 13b shows a trend of increasing number fraction of particles with $D_{dry} < 100$ nm with the decrease of N_{CCN}. It is worth noting that although secondary particle formation and growth events occurred during Gosan 2008, increasing relative deviations or number fraction of particles having $D_{dry} < 100$ nm cannot be attributed to these events since data during these events was only a minor fraction of the total data. Such correlated trends indicate that the over-prediction by Method AR08 is due to assigning κ values that are too high for particles having $D_{dry} < 100$ nm (Fig. 11), which results in false activation of particles that are too small to be activated. Kammermann et al. (2010) also found that κ of 0.3 predicted GF values that were too high and that were rarely measured at that subarctic site. This also explains why the method that uses GF data resulted in much less over-prediction and again demonstrates that hygroscopicity measurements for small aerosols ($D_{dry} < 100$ nm) are important for estimating N_{CCN}.

Based on our data set, however, we may refine Method AR08. The campaign-averaged κ value for 50 and 100 nm particles during Gosan 2008 is 0.17. Therefore, prescribing κ of 0.17 for particles smaller than 100 nm diameter and 0.30 for particles larger than 100 nm diameter can be a good alternative. The result of this refinement (named "Method AR08 refined") is shown in Fig. 13a and indeed it shows almost as good agreement as Method 1 for the Gosan 2008 campaign without the systematic increase of relative deviation with the increase of measured N_{CCN}. However, we would not claim that the refinement suggested here can be applied to all continental environments. More observational data should be accumulated for such an attempt.

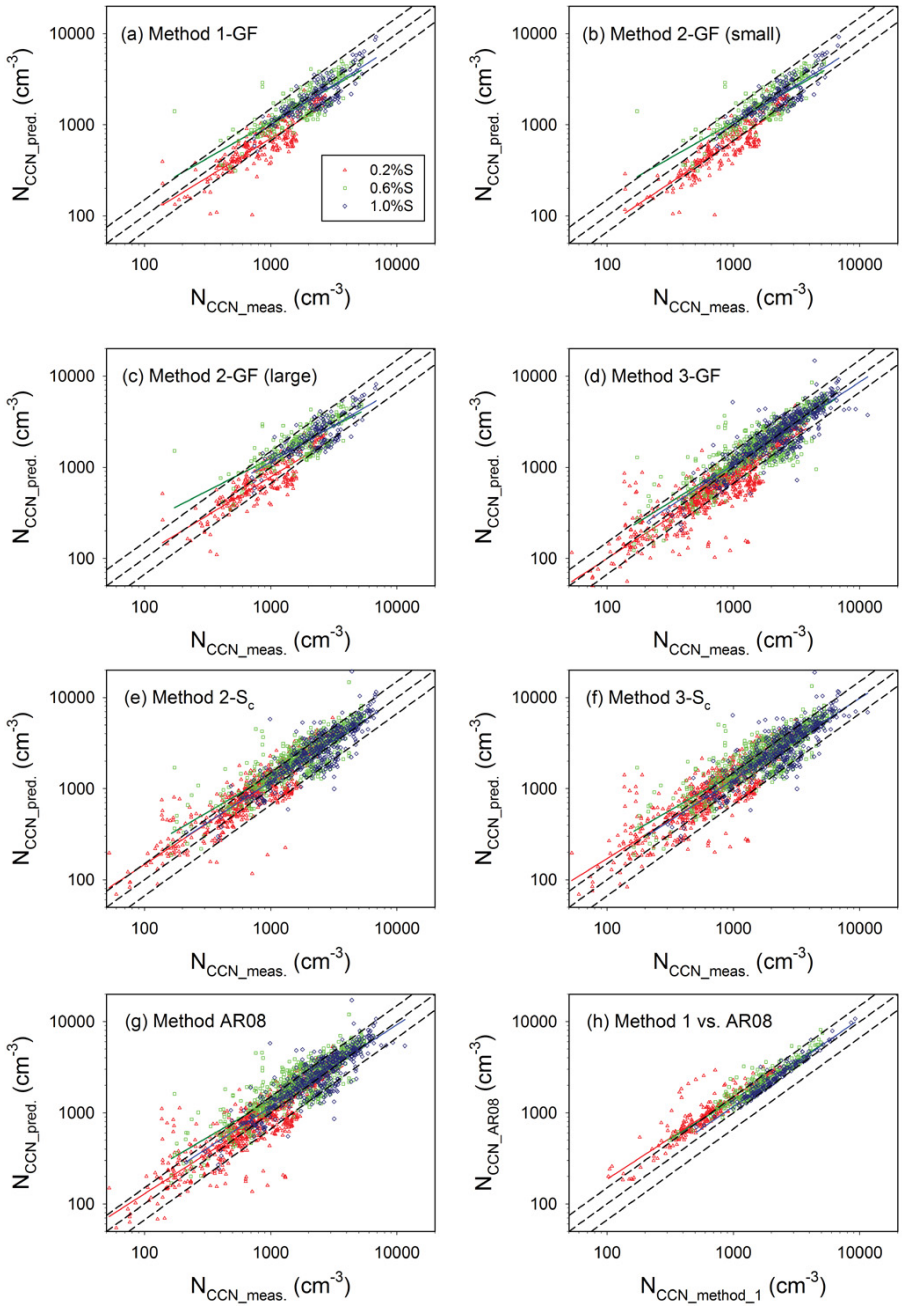

Fig. 12. (a–g) CCN closure results from various methods and **(h)** comparison between Method 1 and Method AR08. For the description of each method, see Table 5. The dotted lines indicate ±50 % error.

5 Summary and conclusion

Aerosol hygroscopic growth factor, CCN spectra and critical supersaturation (S_c) were measured at two remote Korean islands (Gosan, Jeju Island and Baengnyeongdo Comprehensive Monitoring Observatory (BCMO), Baengnyeongdo) along with aerosol concentration and size distribution during four field campaigns held in: August 2006 (Gosan); April–May 2007 (Gosan); August–October 2008 (Gosan) and August 2009 (BCMO). Total aerosol concentrations (N_{CN}) at the two islands were comparable to those measured over the nearby seas, indicating that the local anthropogenic sources within the islands were negligible. However, $PM_{2.5}$, PM_{10}, SO_2, O_3 and CO concentrations measured at the two islands suggested that the two islands were constantly under anthropogenic influences from the Asian continent regardless of the season or year. Average values for all of the measured CCN concentrations (N_{CCN}) at 0.2, 0.6 and 1.0 %

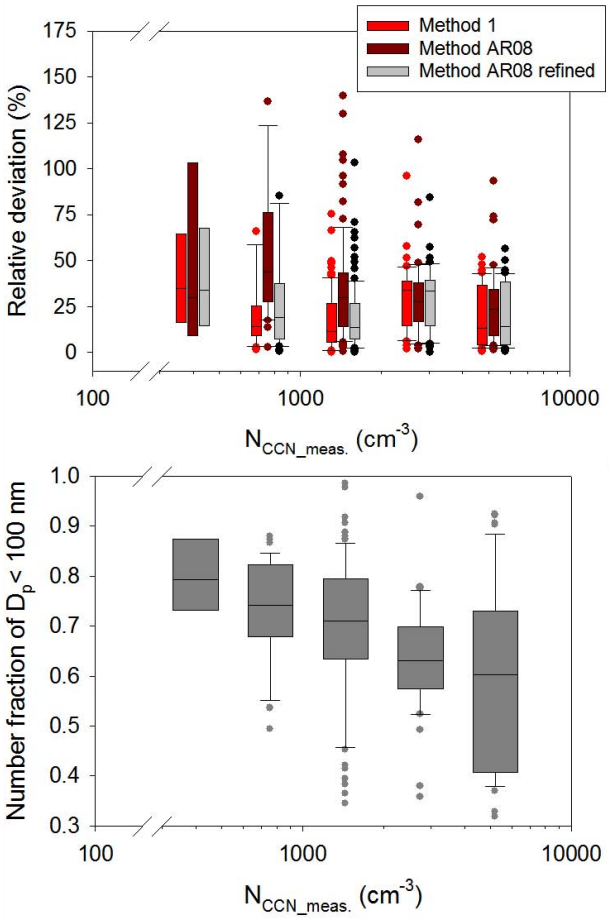

Fig. 13. **(a)** Relative deviations, defined as $|N_{CCN\_pred}N_{CCN\_meas}|/N_{CCN\_meas}$, for methods 1 and 4, and **(b)** the number fraction of particles smaller than 100 nm D_p for each NCCN bin. The schematic plots are drawn in the same manner as explained in Fig. 11.

supersaturation (S), N_{CN} and geometric mean diameter (D_g) from both islands were in the range of 1043–3051 cm^{-3}, 2076–4360 cm^{-3}, 2713–4694 cm^{-3}, 3890–5117 cm^{-3} and 81–98 nm, respectively, and BCMO recorded the highest N_{CCN} for all S when compared to Gosan measurements. Significantly higher SO_2 concentrations at BCMO may be responsible for the high N_{CCN}/N_{CN} for $S \leq 0.6$ as SO_2 is the precursor of sulfates.

The aerosols were mostly internally mixed, although a minor fraction of samples contained externally mixed hydrophobic aerosols. No significant differences in hygroscopicity were found between pollution and non-pollution days at both islands suggesting that continental sources were constantly affecting the sites even on days classified as non-pollution days. Greater hygroscopicity (lower S_c) was measured at BCMO for all sizes compared to Gosan. This is consistent with higher SO_2 of BCMO. Generally, the hygroscopicity measured at the two islands was similar to that measured during ACE-Asia over the sea 500 km east of Gosan but it was significantly higher than that measured at a site downwind of Beijing, indicating that aerosols measured at Gosan might have experienced aging processes during their transport, which added to their hygroscopicity.

During the 2008 and 2009 campaigns, critical supersaturations for CCN activation (S_c) of particles of selected sizes were estimated by size-resolved N_{CCN}/N_{CN} measurements. These S_c values at BCMO were distinctly different depending on whether the air masses came from China (lower S_c) or Korea/Japan (higher S_c). This distinction was not observed at Gosan. By compiling all HTDMA and DMA-CCN measurements that were conducted at Gosan since 2005, we suggest that aerosol hygroscopicity may have decreased during this period. An important result was that hygroscopicity estimated from the S_c measurements was higher than hygroscopicity based on GF measurements. The reason for this is not yet clear.

The temporally varying and size-resolved HTDMA hygroscopicity data predicted N_{CCN} with average relative deviations of 28 ± 20 % (under-prediction dominant), 25 ± 52 (balanced between over- and under-prediction) and 19 ± 15 % (balanced) for 0.2, 0.6 and 1.0 % S, respectively. Comparisons of various CCN closure methods that used HTDMA data suggested that it was crucial to know hygroscopicity of aerosols smaller than 100 nm diameter for accurately predicting N_{CCN}. Prescribing a fixed hygroscopicity value as suggested by Andreas and Rosenfeld (2008) for aged continental aerosols resulted in average relative deviations in the range of 25–40 % with over-prediction dominant. The relative deviation tended to increase with decreasing N_{CCN}, which was accompanied by an increase of the sub-100 nm fraction. Considering the fact that numerical models usually vary N_{CCN} to simulate aerosol effects on clouds, such findings indicate the potential error of using a constant hygroscopicity as a global representative value for aged continental aerosol. Using different hygroscopicities for different particle sizes might be a better way to represent continental CCN distributions in models as demonstrated by the much improved CCN closure when the hygroscopicity value of 0.17 was used for sub-100 nm instead of prescribing the constant hygroscopicity value of 0.3 for all sizes.

Supplementary material related to this article is available online at: http://www.atmos-chem-phys.net/11/12627/2011/acp-11-12627-2011-supplement.pdf.

Acknowledgements. The authors would like to express special thanks to Kimberly Prather of University of California, San Diego, for providing 2007 CN data. Special thanks also go to Mr. Kyung-Sik Kang for providing all the local support during the 2006, 2007 and 2008 Gosan campaigns and to the staffs at BCMO for the 2009 BCMO campaign. The authors would like to thank three anonymous referees for making valuable suggestions, which

led to a great improvement of the manuscript. This work was funded by the Korea Meteorological Administration Research and Development Program under Grant RACS_2010-5001.

Edited by: M. Gysel

References

Adhikari, M., Ishizaka, Y., Minda, H., Kazaoka, R., Jensen, J. B., Gras, G. L., and Nakajima, T.: Vertical distribution of cloud condensation nuclei concentrations and their effect on microphysical properties of clouds over the sea near the southwest islands of Japan, J. Geophys. Res., 110, D10203, doi:10.1029/2004JD004758, 2005.

Andreae, M. O. and Rosenfeld, D.: Aerosol–cloud–precipitation interactions. Part 1. The nature and sources of cloud-active aerosols, Earth-Sci. Rev., 89, 13–41, 2008.

Asmi, A., Wiedensohler, A., Laj, P., Fjaeraa, A.-M., Sellegri, K., Birmili, W., Weingartner, E., Baltensperger, U., Zdimal, V., Zikova, N., Putaud, J.-P., Marinoni, A., Tunved, P., Hansson, H.-C., Fiebig, M., Kivekäs, N., Lihavainen, H., Asmi, E., Ulevicius, V., Aalto, P. P., Swietlicki, E., Kristensson, A., Mihalopoulos, N., Kalivitis, N., Kalapov, I., Kiss, G., de Leeuw, G., Henzing, B., Harrison, R. M., Beddows, D., O'Dowd, C., Jennings, S. G., Flentje, H., Weinhold, K., Meinhardt, F., Ries, L., and Kulmala, M.: Number size distributions and seasonality of submicron particles in Europe 20082009, Atmos. Chem. Phys., 11, 5505–5538, doi:10.5194/acp-11-5505-2011, 2011.

Bates, T. S., Coffman, D. J., Covert, D. S., and Quinn, P. K.: Regional marine boundary layer aerosol size distributions in the Indian, Atlantic, and Pacific Oceans: A comparison of INDOEX measurements with ACE-1, ACE-2, and Aerosol 99, J. Geophys. Res., 107, 8026, doi:10.1029/2001JD001174, 2002.

Brechtel, F. J. and Kreidenweis, S. M.: Predicting particle critical supersaturation from hygroscopic growth measurements in the humidi?ed TDMA. Part I: Theory and sensitivity Studies, J. Atmos. Sci., 57, 1854–1871, 2000.

Cerully, K. M., Raatikainen, T., Lance, S., Tkacik, D., Tiitta, P., Petäjä, T., Ehn, M., Kulmala, M., Worsnop, D. R., Laaksonen, A., Smith, J. N., and Nenes, A.: Aerosol hygroscopicity and CCN activation kinetics in a boreal forest environment during the 2007 EUCAARI campaign, Atmos. Chem. Phys. Discuss., 11, 15029–15074, doi:10.5194/acpd-11-15029-2011, 2011.

Covert, D. S., Kapustin, V. N., Bates, T. S., and Quinn, P. K.: Physical properties of marine boundary layer aerosol particles of the mid-Pacific in relation to sources and meteorological transport, J. Geophys. Res., 101, 6919–6930, 1996.

Cubison, M. J., Ervens, B., Feingold, G., Docherty, K. S., Ulbrich, I. M., Shields, L., Prather, K., Hering, S., and Jimenez, J. L.: The influence of chemical composition and mixing state of Los Angeles urban aerosol on CCN number and cloud properties, Atmos. Chem. Phys., 8, 5649–5667, doi:10.5194/acp-8-5649-2008, 2008.

Dusek, U., Covert, D. S., Wiedensohler, A., Neusüss, C., Weise, D., and Cantrell, W.: Cloud condensation nuclei spectra derived from size distributions and hygroscopic properties of the aerosol in coastal south-west Portugal during ACE-2, Tellus, 55B, 35–53, 2003.

Dusek, U., Frank, G. P., Hildebrandt, L., Curtius, J., Schneider, J.,Walter, S., Chand, D., Drewnick, F., Hings, S., Jung, S., Borrmann, S., and Andreae, M. O.: Size matters more than chemistry for cloud-nucleating ability of aerosol particles, Science, 312, 1375–1378, 2006.

Eichler, H., Cheng, Y. F., Birmili, W., Nowak, A., Wiedensohler, A., Brüggemann, E., Gnauk, T., Herrmann, H., Althausen, D., Ansmann, A., Engelmann, R., Tesche, M., Wendisch, M., Zhang, Y. H., Hu, M., Liu, S., and Zeng, L. M.: Hygroscopic properties and extinction of aerosol particles at ambient relative humidity in South-Eastern China, Atmos. Environ., 42, 6321–6334, 2008.

Ervens, B., Cubison, M. J., Andrews, E., Feingold, G., Ogren, J. A., Jimenez, J. L., Quinn, P. K., Bates, T. S., Wang, J., Zhang, Q., Coe, H., Flynn, M., and Allan, J. D.: CCN predictions using simplified assumptions of organic aerosol composition and mixing state: a synthesis from six different locations, Atmos. Chem. Phys., 10, 4795–4807, doi:10.5194/acp-10-4795-2010, 2010.

Flowers, B. A., Dubey, M. K., Mazzoleni, C., Stone, E. A., Schauer, J. J., Kim, S.-W., and Yoon, S. C.: Optical-chemical-microphysical relationships and closure studies for mixed carbonaceous aerosols observed at Jeju Island; 3-laser photoacoustic spectrometer, particle sizing, and filter analysis, Atmos. Chem. Phys., 10, 10387–10398, doi:10.5194/acp-10-10387-2010, 2010

Gasparini, R., Collins, D. R., Andrews, E., Sheridan, P. J., Ogren, J. A., and Hudson, J. G.: Coupling aerosol size distributions and size-resolved hygroscopicity to predict humidity-dependent optical properties and cloud condensation nuclei spectra, J. Geophys. Res., 111, D05S13, doi:10.1029/2005JD006092, 2006.

Gunthe, S. S., King, S. M., Rose, D., Chen, Q., Roldin, P., Farmer, D. K., Jimenez, J. L., Artaxo, P., Andreae, M. O., Martin, S. T., and Pöschl, U.: Cloud condensation nuclei in pristine tropical rainforest air of Amazonia: size-resolved measurements and modeling of atmospheric aerosol composition and CCN activity, Atmos. Chem. Phys., 9, 7551–7575, doi:10.5194/acp-9-7551-2009, 2009.

Hämeri, K., Väkevä, M., Aalto, P. P., Kulmala, M., Swietlicki, E., Zhou, J., Seidl, W., Becker, E., and O'Dowd, C. D.: Hygroscopic and CCN properties of aerosol particles in boreal forests, Tellus, 53B, 359–379, 2001.

Hobbs, P. V.: Introduction to atmospheric chemistry, 276 pp., Cambridge University Press, 2000.

Hoppel, W. A., Fitzgerald, W., Frick, G. M., and Larson, R. E.: Aerosol size distributions and optical properties found in the marine boundary layer over the Atlantic Ocean, J. Geophys. Res., 95, 3659–3686, 1990.

Hudson, J. G.: An instantaneous CCN spectrometer, J. Atmos. Oceanic Technol., 6, 1055–1065, 1989.

Hudson, J. G.: Variability of the relationship between particle size and cloud-nucleating ability, Geophys. Res. Lett., 34, L08801, doi:10.1029/2006GL028850, 2007.

Hudson, J. G. and Da, X.: Volatility and size of cloud condensation nuclei, J. Geophys. Res., 101, 4435—4442, 1996.

Hudson, J. G. and Yum, S. S.: Maritime-continental drizzle contrasts in small cumuli, J. Atmos. Sci., 58, 915–926, 2001.

Hudon, J. G., Xie, Y., and Yum, S. S.: Vertical distributions of cloud condensation nuclei spectra over the summertime Southern Ocean, J. Geophys. Res., 103, 16609–16624, 1998.

Hudson, J. G., Noble, S., and Jha, V.: Stratus cloud

supersaturations, Geophys. Res. Lett., 37, L21813, doi:10.1029/2010GL045197, 2010.

Huebert, B. J., Bates, T., Russell, P. B., Shi, G., Kim, Y. J., Kawamura, K., Carmichael, G., and Nakajima, T.: An overview of ACE-Asia: Strategies for quantifying the relationships between Asian aerosols and their climatic impacts, J. Geophys. Res., 108, 8633, doi:10.1029/2003JD003550, 2003.

IPCC: Climate Change 2007: The physical science basis. Contribution of Working Group I to the Fourth Assessment Report of the Intergovernmental Panel on Climate Change, edited by: Solomon, S., Qin, D., Manning, M., Chen, Z., Marquis, M., Averyt, K. B., Tignor, M., and Miller, H. L., Cambridge University Press, 2007.

Kammermann, L., Gysel, M., Weingartner, E., Herich, H., Cziczo, D. J., Holst, T., Svenningsson, B., Arneth, A., and Baltensperger, U.: Subarctic atmospheric aerosol composition: 3. Measured and modeled properties of cloud condensation nuclei, J. Geophys. Res., 115, D04202, doi:10.1029/2009JD012447, 2010.

Kaneyasu, N.: Long-term measurement of aerosols on a remote island in the Northwest Pacific Ocean, International Aerosol Conference 2010, Helsinki, Finland, International Aerosol Research Assembly, 2010.

Khain, A., Ovtchinnikov, M., Pinsky, M., Pokrovsky, A., and Krugliak, H.: Notes on the state-of-the-art numerical modeling of cloud microphysics, Atmos. Res., 55, 159–224, 2000.

Kim, J. H., Yum, S. S., Lee, Y.-G., and Choi, B.-C.: Ship measurements of submicron aerosol size distributions over the Yellow Sea and the East China Sea, Atmos. Res., 93, 700–714, 2009a.

Kim, S. K., Kong, B. J., Park, J. S., Lee, S. D., Kim, J. S., and Lee, S. J.: The characteristic of particle composition at Baengnyeong Island, Technical report of National Institute of Environmental Research, NO. 2009-45-1101, 2009b (in Korean with English abstract).

Kim, S.-W., Yoon, S.-C., Jefferson, A., Ogren, J. A., Dutton, E. G., Won, J.-G., Ghim, Y. S., Lee, B.-I., and Han J.-S.: Aerosol optical, chemical and physical properties at Gosan, Korea during Asian dust and pollution episodes in 2001, Atmos. Environ., 39, 39–50, 2005.

Knutson, E. O. and Whitby, K. T.: Aerosol classification by electric mobility: Apparatus, theory, and applications, J. Aerosol. Sci., 6, 443–451, 1975.

Kreidenweis, S. M., Koehler, K., DeMott, P. J., Prenni, A. J., Carrico, C., and Ervens, B.: Water activity and activation diameters from hygroscopicity data – Part I: Theory and application to inorganic salts, Atmos. Chem. Phys., 5, 1357–1370, doi:10.5194/acp-5-1357-2005, 2005.

Kumala, M., Vehkamäki, H. Petäjä, T., Dal Maso, M., Lauri, A., Kerminen, V.-M., Birmili, W., and McMurry, P. H.: Formation and growth rates of ultrafine atmospheric particles: a review of observations, J. Aerosol Sci., 35, 143–176, 2004.

Kuwata, M. and Kondo, Y.: Dependence of size-resolved CCN spectra on the mixing state of nonvolatile cores observed in Tokyo, J. Geophys. Res., 113, D19202, doi:10.1029/2007JD009761, 2008.

Kuwata, M., Kondo, Y., Miyazaki, Y., Komazaki, Y., Kim, J. H., Yum, S. S., Tanimoto, H., and Matsueda, H.: Cloud condensation nuclei activity at Jeju Island, Korea in spring 2005, Atmos. Chem. Phys., 8, 2933–2948, doi:10.5194/acp-8-2933-2008, 2008.

Lance, S., Nenes, A., Mazzoleni, C., Dubey, M. K., Gates, H., Varutbangkul, V., Rissman, T. A., Murphy, S. M., Sorooshian, A., Flagan, R. C., Seinfeld, J. H., Feingold, G., and Jonsson, H. H.: Cloud condensation nuclei activity, closure, and droplet growth kinetics of Houston aerosol during the Gulf of Mexico Atmospheric Composition and Climate Study (GoMACCS), J. Geophys. Res., 114, D00F15, doi:10.1029/2008JD011699, 2009.

Lee, M., Song, M., Moon, K. J., Han, J. S., Lee, G., and Kim, K.-R.: Origins and chemical characteristics of fine aerosols during the northeastern Asia regional experiment (Atmospheric Brown Cloud–East Asia Regional Experiment 2005), J. Geophys. Res., 112, D22S29, doi:10.1029/2006JD008210, 2007.

Massling, A., Leinert, S., Wiedensohler, A., and Covert, D.: Hygroscopic growth of sub-micrometer and one-micrometer aerosol particles measured during ACE-Asia, Atmos. Chem. Phys., 7, 3249–3259, doi:10.5194/acp-7-3249-2007, 2007.

Massling, A., Stock, M., Wehner, B., Wu, Z. J., Hu, M., Brüggemann, E., Gnauk, T., Herrmann, H., and Wiedensohler, A.: Size segregated water uptake of the urban submicrometer aerosol in Beijing, Atmos. Environ., 43, 1578–1589, 2009.

Matsumoto, K., Tanaka, H., Nagao, I., and Ishizaka, Y.: Contribution of particulate sulfate and organic carbon to cloud condensation nuclei in the marine atmosphere, Geophys. Res. Lett., 24, 665–658, 1997.

Mochida, M., Nishita-Hara, C., Kitamori, Y., Aggarwal, S. G., Kawamura, K., Miura, K., and Takami, A.: Size-segregated measurements of cloud condensation nucleus activity and hygroscopic growth for aerosols at Cape Hedo, Japan, in spring 2008, J. Geophys. Res., 115, D21207, doi:10.1029/2009JD013216, 2010.

Nakajima, T., Yoon, S.-C., Ramanathan, V., Shi, G.-Y., Takemura, T., Higurashi, A., Takamura, T., Aoiki, K., Sohn, B.-J., Kim, S.-W., Tsuruta, H., Sugimoto, N., Shimizu, A., Tanimoto, H., Sawa, Y., Lin, N.-H., Lee, C.-T., Goto, D., and Schutgens, N.: Overview of the Atmospheric Brown Cloud East Asian Regional Experiment 2005 and a study of the aerosol direct radiative forcing in east Asia, J. Geophys. Res., 112, D24S91, doi:10.1029/2007JD009009, 2007.

Petters, M. D. and Kreidenweis, S. M.: A single parameter representation of hygroscopic growth and cloud condensation nucleus activity, Atmos. Chem. Phys., 7, 1961–1971, doi:10.5194/acp-7-1961-2007, 2007.

Petters, M. D. and Kreidenweis, S. M.: A single parameter representation of hygroscopic growth and cloud condensation nucleus activity – Part 2: Including solubility, Atmos. Chem. Phys., 8, 6273–6279, doi:10.5194/acp-8-6273-2008, 2008.

Pringle, K. J., Tost, H., Pozzer, A., Pöschl, U., and Lelieveld, J.: Global distribution of the effective aerosol hygroscopicity parameter for CCN activation, Atmos. Chem. Phys., 10, 5241–5255, doi:10.5194/acp-10-5241-2010, 2010.

Pruppacher, H. R. and Klett, J. D.: Microphysics of Clouds and Precipitation, 954 pp., Springer, New York, 1997.

Ramana, M. V., Ramanathan, V., Feng, Y., Yoon, S.-C., Kim, S.-W., Carmichael, G. R., and Schauer, J. J.: Warming in?uenced by the ratio of black carbon to sulphate and the black-carbon source, Nature Geosci., 3, 542–545, doi:10.1038/ngeo918, 2010.

Roberts, G. C. and Nenes, A.: A continuous-flow streamwise thermal-gradient CCN chamber for atmospheric measurements,

Aerosol Sci. Tech., 39, 206–221, 2005.

Rose, D., Gunthe, S. S., Mikhailov, E., Frank, G. P., Dusek, U., Andreae, M. O., and Pöschl, U.: Calibration and measurement uncertainties of a continuous-flow cloud condensation nuclei counter (DMT-CCNC): CCN activation of ammonium sulfate and sodium chloride aerosol particles in theory and experiment, Atmos. Chem. Phys., 8, 1153–1179, doi:10.5194/acp-8-1153-2008, 2008.

Rose, D., Nowak, A., Achtert, P., Wiedensohler, A., Hu, M., Shao, M., Zhang, Y., Andreae, M. O., and Pöschl, U.: Cloud condensation nuclei in polluted air and biomass burning smoke near the mega-city Guangzhou, China – Part 1: Size-resolved measurements and implications for the modeling of aerosol particle hygroscopicity and CCN activity, Atmos. Chem. Phys., 10, 3365–3383, doi:10.5194/acp-10-3365-2010, 2010.

Schwartz, S. E., Charlson, R. J., Khan, R. A., Ogren, J. A., and Rodhe, H.: Why Hasn't Earth Warmed as Much as Expected?, J. Climate, 23, 2453–2464, 2010.

Stith, J. L., Ramanathan, V., Cooper, W. A., Roberts, G. C., DeMott, P. J., Carmichael, G., Hatch, C. D., Adhikary, B., Twohy, C. H., Rogers, D. C., Baumgardner, D., Prenni, A. J., Campos, T., Gao, R., Anderson, J., and Feng, Y.: An overview of aircraft observations from the Pacific Dust Experiment campaign, J. Geophys. Res., 114, D05207, doi:10.1029/2008JD010924, 2009.

Su, H., Rose, D., Cheng, Y. F., Gunthe, S. S., Massling, A., Stock, M., Wiedensohler, A., Andreae, M. O., and Pöschl, U.: Hygroscopicity distribution concept for measurement data analysis and modeling of aerosol particle mixing state with regard to hygroscopic growth and CCN activation, Atmos. Chem. Phys., 10, 7489–7503, doi:10.5194/acp-10-7489-2010, 2010.

Swietlicki, E., Zhou, J., Berg, O. H., Martinsson, B. G., Frank, G., Cederfelt, S.-I., Dusek, U., Berner, A., Birmili, W., Wiedensohler, A., Yuskiewicz, B., and Bower, K. N.: A closure study of sub-micrometer aerosol particle hygroscopic behavior, Atmos. Res., 50, 205–240, 1999.

Swietlicki, E., Hansson, H.-C., Hämeri, K., Svenningsson, B., Massling, A., McFiggans, G., McMurry, P. H., Petäjä, T., Tunved, P., Gysel, M., Topping, D., Weingartner, E., Baltensperger, U., Rissler, J., Wiedensohler, A., and Kulmala, M.: Hygroscopic properties of submicrometer atmospheric aerosol particles measured with H-TDMA instruments in various environments – a review, Tellus, 60B, 432–469, 2008.

Vestin, A., Rissler, J., Swietlicki, E., Frank, G. P., and Andreae, M. O.: Cloud-nucleating properties of the Amazonian biomass burning aerosol: Cloud condensation nuclei measurements and modeling, J. Geophys. Res., 112, D14201, doi:10.1029/2006JD008104, 2007.

Wang, J., Cubison, M. J., Aiken, A. C., Jimenez, J. L., and Collins, D. R.: The importance of aerosol mixing state and size-resolved composition on CCN concentration and the variation of the importance with atmospheric aging of aerosols, Atmos. Chem. Phys., 10, 7267–7283, doi:10.5194/acp-10-7267-2010, 2010.

Wex, H., McFiggans, G., Henning, S., and Stratmann, F.: Influence of the external mixing state of atmospheric aerosol on derived CCN number concentrations, Geophys. Res. Lett., 37, L10805, doi:10.1029/2010GL043337, 2010.

Wiedensohler, A., Cheng, Y. F., Nowak, A., Wehner, B., Achtert, P., Berghof, M., Birmili, W., Wu, Z. J., Hu, M., Zhu, T., Takegawa, N., Kita, K., Kondo, Y., Lou, S. R., Hofzumahaus, A., Holland, F., Wahner, A., Gunthe, S. S. Rose, D., Su, H., and Pöschl, U.: Rapid aerosol particle growth and increase of cloud condensation nucleus activity by secondary aerosol formation and condensation: A case study for regional air pollution in northeastern China, J. Geophys. Res., 114, D00G08, doi:10.1029/2008JD010884, 2009.

Yum, S. S., Hudson, J. G., and Xie, Y.: Comparisons of cloud microphysics with cloud condensation nuclei spectra over the summertime Southern Ocean, J. Geophys. Res., 103, 16625–16636, 1998.

Yum, S. S. and Hudson, J. G.: Vertical distributions of cloud condensation nuclei spectra over the springtime Arctic Ocean, J. Geophys. Res., 106, 15045–15052, 2001.

Yum, S. S. and Hudson, J. G.: Maritime/continental microphysical contrasts in stratus, Tellus, 54B, 61–73, 2002.

Yum, S. S., Hudson, J. G., Song, K. Y., and Choi, B.-C.: Springtime cloud condensation nuclei concentrations on the west coast of Korea, Geophys. Res. Lett., 32, L09814, doi:10.1029/2005GL022641, 2005.

Yum. S. S., Roberts, G., Kim, J. H., Song, K., and Kim, D.: Submicron aerosol size distributions and cloud condensation nuclei concentrations measured at Gosan, Korea, during the Atmospheric Brown Clouds-East Asian Regional Experiment 2005, J. Geophys. Res., 112, D22S32, doi:10.1029/2006JD008212, 2007.

Zhou, J., Swietlicki, E., Hansson, H. C., and Artaxo, P.: Submicrometer aerosol particle size distribution and hygroscopic growth measured in the Amazon rain forest during the wet season, J. Geophys. Res., 107, 8055, doi:10.1029/2000JD000203, 2002.